

Demonstration of Excess Correlation in Non-Local Random Number Generators Sharing Circular, Changing Angular Velocity Magnetic Fields

Lyndon M. Juden-Kelly^{1,2}, Blake T. Dotta^{1,3}, David A. E. Vares^{1,2}
& Michael A. Persinger^{1,2,3*}

Neuroscience Research Group¹, Human Studies² and Biomolecular Sciences³ Programs,
Laurentian University, Sudbury, Ontario, Canada P3E 2C6

ABSTRACT

To test if temporally-coupled diametric shifts in parity could be demonstrated for non-local distances between “random” events generated by electron tunnelling-based circuits, two REG (Random Event Generators) were each exposed within a circular array of solenoids separated by 10 m. Each circular array generated a patterned rotating magnetic field that has previously produced transient excess correlation and entanglement in photon reactions and alterations in pH in spring water. During a 30 min interval the REGs were exposed first to an accelerating group velocity embedded with a diminishing frequency/phase-modulated field (the primer) followed by a decelerating group velocity embedded with an increasing frequency/phase-modulated magnetic field (the effector). Only after exposures for about 4 min to the second (effector) condition that is known to manifest the effects of entanglement did the random numbers deviate significantly and by more than one standard deviation in an opposite direction to each other. The estimated increments of energy were between 10^{-21} and 10^{-20} J which is within the range of the energy derived from the universe’s total force per Planck’s voxel distributed over the distance of the hydrogen wavelength. These results indicate that excess correlation can be generated within “random”, quantum electronic processes whose spatial domains are similar to neuronal synapses at the macro-level by appropriate applications of weak, microTesla level, magnetic fields.

Keywords: Entanglement, random event generators, circular rotating magnetic fields, excess correlations.

1. Introduction

Entanglement, frequently studied since the term was first introduced by Erwin Schrodinger (Aczel, 2002), is still considered a mystery with respect to mechanism and explanation. Traditionally excess correlation between two particles representative of entanglement has been restricted to photons or to clusters of photons (Vaziri et al, 2002). Considering the intricate relationship between photons as quanta of energy and shifts in electron

*Corresponding author: Dr. M. A. Persinger, mpersinger@laurentian.ca

shells, one would expect that phenomena that involve the movement of electrons across specific geometries, such as p-n junctions, might also exhibit this capacity.

Many REGs (Random Event Generators) employ these mechanisms in order to discern if proximal stimuli can affect “random distributions” of 0, 1 outcomes. If the electron tunnelling processes associated with REG operations that produce 0, 1 series of numbers are similar to that of parity in paired, entangled photons, then there should be an elementary test of this manifestation of excess correlation. If the two (REG) systems are “entangled” then a deviation in one direction of “randomicity” exhibited by one REG should occur co-temporally with a deviation in the other direction of randomicity in the coupled second REG. Here we present experimental evidence for this effect.

The operational essence of entanglement that leads to excess correlations is that two loci share specific physical parameters in space-time. The two loci then respond as if they occupy the identical space-time field. One interpretation is that superposition has resulted in a virtual juxtaposition and transposition of the two loci’s axes. The concept is an extension of Mach’s principle which suggested that all particles in the universe are relatable by their (angular) momentum or their moments of inertia. As a result every particle in the universe is affected by all other particles in the universe. The movement of an electromagnetic field around a circle is a special condition because of the angular velocity and its implicit constant “acceleration”.

When a packet of particles are moving through space time there are two components. The first is the group velocity; the second is the phase velocity of the particles within the group. If the two are equal then there are no interference or birefringence patterns. Tu et al (2005) has strongly suggested that if these packets of particles are photons and there is a discrepancy between the group and phase velocity then a non-zero mass emerges for the photons. One of the consequences is the emergence of a third direction of the photon. The other directly applicable consequence is that the product of the upper limit of the rest mass of a photon ($\sim 2 \cdot 10^{-52}$ kg), the entanglement velocity (Persinger and Koren, 2013) of $2.8 \cdot 10^{23} \text{ m} \cdot \text{s}^{-1}$, and the velocity of light in a vacuum ($3 \cdot 10^8 \text{ m} \cdot \text{s}^{-1}$) is $\sim 1.7 \cdot 10^{-20} \text{ J}$.

The 10^{-20} J is a value that emerges when the total force within the universe is divided by the sum of Planck’s voxels that comprise its volume and the force is then applied across the wavelength of the neutral hydrogen line (Persinger, 2015). This is the quantum associated with a single action potential of an axon as well as the energy from the force between potassium ions that contribute to the resting membrane potential of the plasma cell membrane. It is also within the range of the increment of energy known to be associated at the fundamental level with the electron tunnelling within the type of p-n junctions within the REGs. The convergences would be consistent with the conditions required for phenomena that exhibit properties of entanglement.

Dotta and Persinger (2012) applied this concept to an experimental setting whereby pulsing magnetic fields generated through optocoupler systems to circular arrays of 8 pairs of solenoids were uncoupled with respect to phase and group velocity. The group velocity which was the changing angular velocity as the magnetic field rotated around the circular arrays of solenoids and the phase velocity, defined as the shifting frequency and phase modulation of the complex pattern that composed the magnetic field, differed. When two bioluminescent reactions were placed in the center of each of the two circular arrays separated by 10 m a doubling of

photon emission (as if the two loci had been superimposed) occurred if they were first exposed to an accelerating group velocity embedded with a decreasing phase velocity and then to a decreasing group velocity embedded with an increasing phase velocity. These were called the primer and effector fields, respectively. Reversal of the presentations of the sequence, coupled phase-group velocity fields, or no changing angular velocity, did not produce the “doubling” of photons.

The effect was also observed in spring water within which diametrically opposite shifts occurred in pH within the two distant spaces surrounded by the rings of solenoids. In a series of 24 experiments; inverse shifts in pH were noted in two quantities of spring water separated by 10 meters that shared rotating magnetic fields with changing angular velocities when one solution was injected with proton donors (weak acetic acid). It was also found that the associated fixed amount of energy of 10^{-20} J 10^{-21} J per molecule from the coordinated fields in the two loci was related to the change in numbers of H^+ within these volumes and predicted the time required to produce the maximum shift in pH (Dotta et al., 2013).

Excess correlation is not exclusive to pH shifts in water but also applies to electron spins and gases (Ahn et al., 2000; Fickler et al., 2012; Hoffman et al., 2012; Julsaarg et al., 2001). Excess correlation has been found up to 300 km between pairs of brains that shared circularly rotating magnetic fields from a different technology where the fields were generated through cerebral toroids driven by Ardueno circuits maintained by laptop computers. Discrete changes in QEEG (quantitative electroencephalographic) power within the cerebral space of a non-local subject was experimentally demonstrated when the pair were exposed to specific configurations of circular magnetic fields with changing angular velocities that dissociated the phase and group components. These non-local discrete changes in power occurred when the local participant was exposed to sound pulses but not light flash frequencies (Burke et al., 2013).

The signal to noise ratio and inferences of manifestation within excess correlations with regard to human cerebrums seems to be heightened when the pairs of individuals have had proximal space-time relations from previous relations. When ‘pairs’ of individuals were separated by 75 m, ~50% of the variance of the “simultaneous” electroencephalographic power was shared between the pairs of brains. Positive correlations were found within the alpha and gamma bands within the temporal and frontal lobes. However the alpha and theta bands were found to be negatively correlated for pairs of people who had a protracted history of interaction (Dotta et al., 2009). This would be consistent with a more macro-entanglement of the frequent observation that if the parity of one entangled photon is changed the other changes in the opposite direction.

2. Theory and Presumed Operation of the RNG

The RNG (Random Number Generator) or REG (Random Event Generator) device was purchased from Psyleron Inc. (hardware ID: RGZD750) and is designed to generate random numbers based on quantum principles. As described Psyleron’s technicians and by Vares and Persinger (2013), two environmentally shielded, Fairchild NPN Epitaxial 0.048mg Silicon Transistors (BCX70K), under a reversed biased current employed heavily doped electrons to

quantum tunnel across a classical channel barrier. The authors assume the proprietary distance of the gap junction barrier is of the order of the industry about 1 μm with a functional width of similar magnitude. Following the Heisenberg Uncertainty Principle, the probability of an electron randomly occurring on the opposite side of the gap junction channel barrier, translates into a varying voltage level.

The varying voltage (white noise) generated by quantum tunnelling electrons is sampled from a reverse-biased ‘Field Effect Transistor’ (FET). The unpredictably ‘high’ and ‘low’ voltages are due to more or less electrons tunnelling across the barrier (gap junction), with a spectrum +/- 1dB, from 50Hz to 20kHz. A 1 kHz cut-off attenuates frequencies, followed by filtering, transistor signal amplification and clipping to produce a rectangular wave. Gated sampling at an approximate constant 1-kHz rate yields a regularly spaced sequence of random bits. To eliminate environmental biases, the two streams from both chips undergo Boolean Exclusive-OR logic gate operation procedures, whereby: [(1 XOR 1 = 0), (1 XOR 0 = 1), (0 XOR 1 = 1), and (0 XOR 0 = 0)] respectively. Further, the entire circuit is shielded by an outer aluminum enclosure, as well as with an inner perm alloy mu-metal which isolates both electrical and magnetic effects from inside and outside the REG device. In short, the Psyleron REG is a professional, non-classical coin flipper with data accessed by computer via USB port.

Leo Esaki (1958) noted that the current in the reverse diode might only be carried by internal field emission. The barrier breakdown occurs at less than the threshold voltage for electron-hole pair production, and so an avalanche should be excluded. Due to the extensive shielding and calibration testing of the Psyleron REG-1 device, classical physical interactions can be ruled out as the source of deviation from statistical randomness. The velocity of an incident tunnelling electron wave packet becomes infinite inside a zero-time space barrier. With wave number k imaginary, the duration of time for the incident electron wave packet to tunnelling across the potential barrier approaches zero. We have assumed, based upon the diffusivity velocity calculated by Persinger and Koren (2013), that the value is very fast but non-zero. If the manifestation of entanglement velocity is $2.8 \cdot 10^{23} \text{ m} \cdot \text{s}^{-1}$, the time required to traverse p-n junction of $\sim 1 \text{ } \mu\text{m}$ would be $0.3 \cdot 10^{-29} \text{ s}$. This tunnelling phase change is a special solution of the Schrodinger wave function:

$$\psi_I(x, t) = e^{-\frac{iEt}{\hbar}} \left[A_I e^{\frac{ipx}{\hbar}} + B_I e^{-\frac{ipx}{\hbar}} \right] \quad (1)$$

where; particle momentum $p = (\sqrt{2mE})$, A_I and B_I are Eigen functions of the momentum operators for the incident and reflected propagations of the particle in each region. During tunnelling in the barrier region (II), the corresponding wave function solution ψ_{II} undergoes absorption. Although the energy of the instantaneously tunnelled electron remains consistent, the probability amplitude is no longer the simple addition of oscillating functions, but combinations of exponential ones (Hartman, 1962). There exists the quantum wave function state possibility of a transition of electrons from the valence band, into quantum states of like energy in the conduction band. Quantum tunnelling is therefore known as the finite probability, as determined by the ratio of coefficients of the special Schrodinger equation, of finding instantaneous particles at the instantaneous inflection points between discrete regions.

The phase change solutions to the special Schrodinger equations violate Einstein causality for signal transmissions through a vacuum. For: $(W^2 = c^2 p^2)$ where: $W = (\text{energy})$, and

p = (momentum), the instantaneous tunnelling electron is faster than the speed of light. However when the entanglement velocity is assumed and the traversal time is $0.3 \cdot 10^{-29}$ s, the equivalent frequency is $3.3 \cdot 10^{29}$ Hz and hence the energy of the wave packet would be the multiplication by Planck's constant ($6.626 \cdot 10^{-34}$ J·s) or $\sim 22 \cdot 10^{-5}$ J. When divided by the rest mass ($9.1 \cdot 10^{-31}$ kg) of 10^{10} electrons ($9.1 \cdot 10^{-21}$ kg), the estimated numbers involved with the expected density of silicon molecules on each surface between the barriers, the remaining value is $2.4 \cdot 10^{16}$ $\text{m}^2 \cdot \text{s}^{-2}$ or $1.6 \cdot 10^8$ $\text{m} \cdot \text{s}^{-1}$. This is very convergent with the velocity of light. Hence if the tunnelling duration is assumed to be a non-zero value which is the entanglement velocity the resulting energy values for a specific aggregate of electron masses moving coherently resolves as the velocity of light in that domain. This functional equivalence between the photonic property and the aggregate of electrons that displays one wave function for the whole system (Ψ) and not separate waves for each particle also suggests that the electron tunnelling *process* might be entangled experimentally.

Considering the fluctuations are quantum in nature, literature investigation revealed a laboratory device that measures quantum vacuum fluctuations (Symul et. al., 2011). A laser is split, and two homodyne photodetectors measure the difference. Electronic noise was filtered to reveal inherent vacuum fluctuation measures which were then sourced to create quantum random numbers. Modern measuring techniques use a charge coupled device (CCD) to measure vacuum fluctuations, a review of their structure, and that semiconductors are light sensitive, indicate a similar p-n junction as the RNG device. The baseline means per second for one of these devices that operated continually for one month was 99.9945. The standard deviation was 0.1228 and the minimum and maximum was 99.6606 to 100.3397.

3. Methods

A total of 9 trials were complete over a 25 day period. The experimental procedure involved two Random Event Generators (REG's) and two custom-constructed "Octopus" devices (Dotta and Persinger, 2012) each composed of circular arrays of 8 pairs of solenoids and located in two remote locations within the Consciousness lab at Laurentian University. The first location, designated as "local" was an industrial acoustic chamber. The second location was another room approximately 10 m away. The designation for this experiment was arbitrary because there was no stimulation or experimental manipulation in one locus to discern the inverse response in the other locus. We assumed the opposing polarity would occur "spontaneously" due to the nature of entanglement. The object of the experiment was to discern the fluctuation in putatively "random" processes from the level of quantum operations across p-n junction tunnelling and to measure the change when the consequences of entanglement had occurred. The REG devices were placed in the center of the array solenoids as shown in Figure 1.

The Experimental REG 'Entanglement' procedure was identical to the procedure employed by Dotta and Persinger (2012) to produce the "doubling" of photon emissions from chemiluminescent reactions when both reactions were exposed to the same circularly, rotating magnetic fields. In their study the entanglement occurred during the second (effector) pattern after the presentation of a specific (primer) pattern had been presented. The field strength within the center of the ring of solenoids, where the Psyleron sensors were placed, was ~ 1 uT.

The sequence of presentations employed in the present study which was identical to the Dotta and Persinger (2012) sequence included nine 2 minute conditions spaced by 1 minute intervals which commenced in the following order: Baseline 1 (BL1), Baseline 2 (BL2), Thomas 1 (T1), Thomas 2 (T2), Burst-X 1 (B1), Burst-X 2 (B2), Burst-X 3 (B3), Baseline 3 (BL3), Baseline 4 (BL4). These terms refer to the names attributed to the pattern of the field generated by the computer that was delivered sequentially to each solenoid.

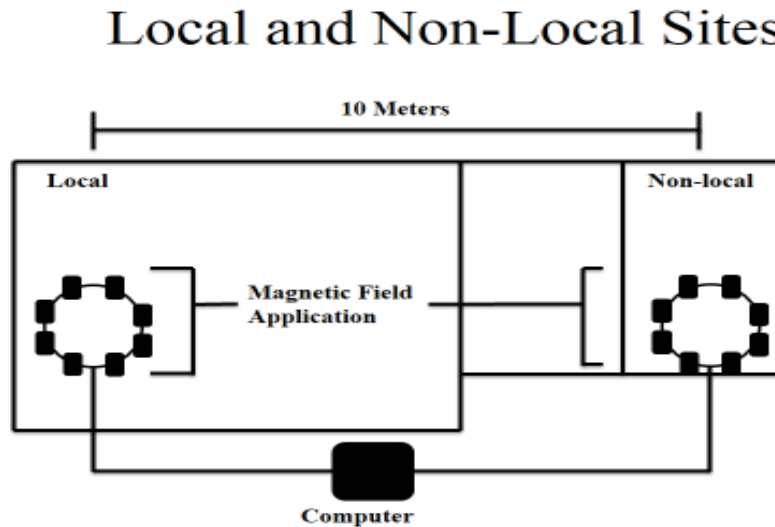


Figure 1. Diagram of the experimental arrangement. The two circular arrays of pairs of solenoids are indicated by the rings. The rate of rotation (counterclockwise from the top) and the accelerating or decelerating phase patterns were generated by the programmable software from the computer. Each REG was placed within the center of one of the coils. The location of each REG was counterbalanced over the 9 trials.

The Thomas pattern was a decelerating frequency or “phase” modulated pattern composed of 839 points. The shape has been published elsewhere Dotta and Persinger (2012). The Burst-X pattern was an accelerating frequency or phase modulated pattern composed of 230 points. The designation number (suffix) refers to the partitioning of the time for analyses in order to discern consistency of any effect as well as their potential transience.

All point durations that composed the patterns were 1 ms. This duration was based upon the calculation by Persinger and Koren (2007) for the hypothetical time, derived from Hubble’s Parameter, for an electron to expand one Planck’s Length. This meant that the value between 0 and 256 from the column of numbers from which the patterns were generated were converted into a value between -5 V and +5 V (127 = 0 V) for 1 ms (plus the port time) from the IBM 286 computer. The Thomas pattern was generated through the pairs of solenoids in each of the 8 positions as they were activated with an accelerating angular velocity. The duration of the field in the first solenoid was 20 ms and was decreased by 2 ms for each successive solenoid in the ring until the final duration in the 8th solenoid was 6 ms. We described this the primer field where the uncoupled group and phase velocity resulted in an increasing group velocity (the rotating speed) and a decreasing phase velocity.

The Burst-x pattern produced a temporally opposing effect. It was generated within each solenoid, starting with 20 ms, but increased in duration by 2 ms until by the 8th solenoid the duration was 34 ms. We described this field as the effector field, where the display of “excess correlation” is clearly evident. During this condition the “group velocity” was decreasing while the phase velocity was increasing. We reasoned that if a discrete shift in space and the energy within it mediated the effects of “excess correlation” in this paradigm, any deviation from random variation in the REG outputs should occur during this phase. The REG’s were synchronized through stop watches which ran continuously throughout the experiment after being synchronized. All field conditions had 1,1 delay between points and point duration presentations. Several variables were collected from each REG in each condition including; Overall Z-score, Mean, Standard Deviation, Max/Min Z-score value and min/max z-scores.

4. Results

The results were clear and conspicuous. As shown in Figure 2, the means and standard deviations for the two random numbers clustered around the average of 100. There was no statistically significant differences between the local and non-local sites except for the period during the *middle* of the burst-x (2) field which is the effector field where excess correlations have been observed for luminescent and pH reactions in previous experiments. This would be about 4 min after the “entanglement” field began. As predicted by “entanglement” principles, the shift in the random number generation was significantly in the opposite direction (no overlap of standard deviations) during this interval. The effect was maintained for about 4 min and was not evident in the third burst-x segment.

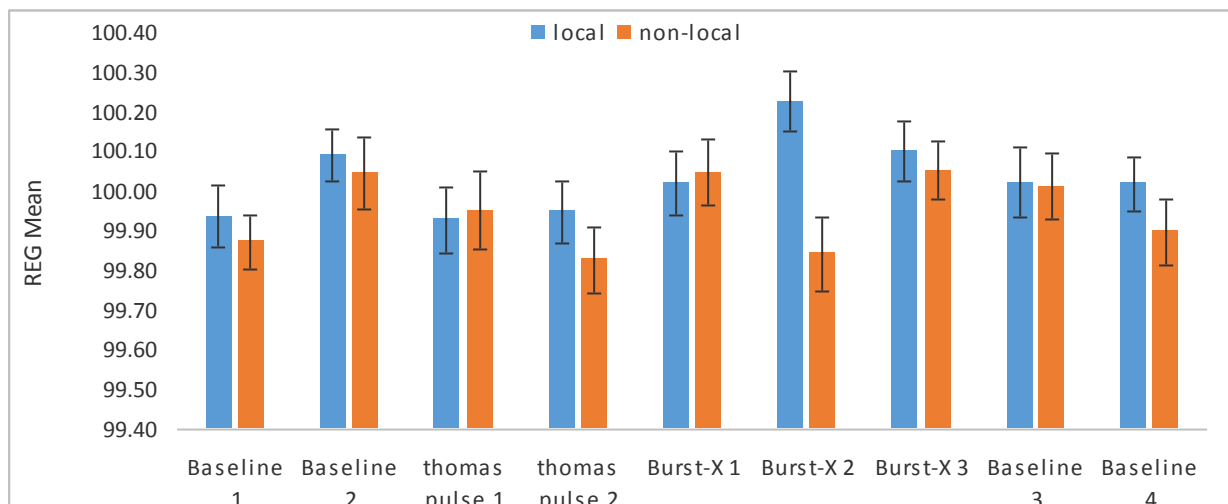


Figure 2. Means and standard deviations for the average numbers of 0s and 1s generated by the two REG in the local (chamber) and non-local room (10 m away) over the various baseline and magnetic field configuration presentations. The local designation was an arbitrary reference. The Thomas pulse is now called the primer pulse while the burst-x pattern is called the effector pulse within which entanglement is usually manifested. The effect was transient but powerful in the center of the entanglement interval (Burst-X2). Vertical bars are standard errors of the mean (SEM).

5. Discussion

The consequence of entanglement (Aczel, 2002) is that two particles are “connected” such that when one of the pairs changes an indicator of polarity, the other member of the pair responds in the opposite direction. This could be considered a higher order manifestation of Newton’s Third Law where ever force (action) displays an equal and opposite force (reaction). Such entanglement, which has been considered central for quantum communication (Vaziri, et al, 2002) is assumed to be restricted to photons. In the present study photonic-energies cannot be excluded because electron tunnelling and the p-n junctions associated with this process involves energies that could facilitate photon involvement. Caswell et al (2014) had shown experimentally that cerebral biophotons could be the potential mediator for non-local human-machine interactions. It may be relevant that the product of the rest mass of a photon ($\sim 2 \cdot 10^{-52}$ kg) the entanglement velocity ($2.8 \cdot 10^{23}$ m·s⁻¹) and the velocity of light ($3 \cdot 10^8$ m·s⁻¹) is $1.7 \cdot 10^{-20}$ J which is well within the energy associated with each action potential.

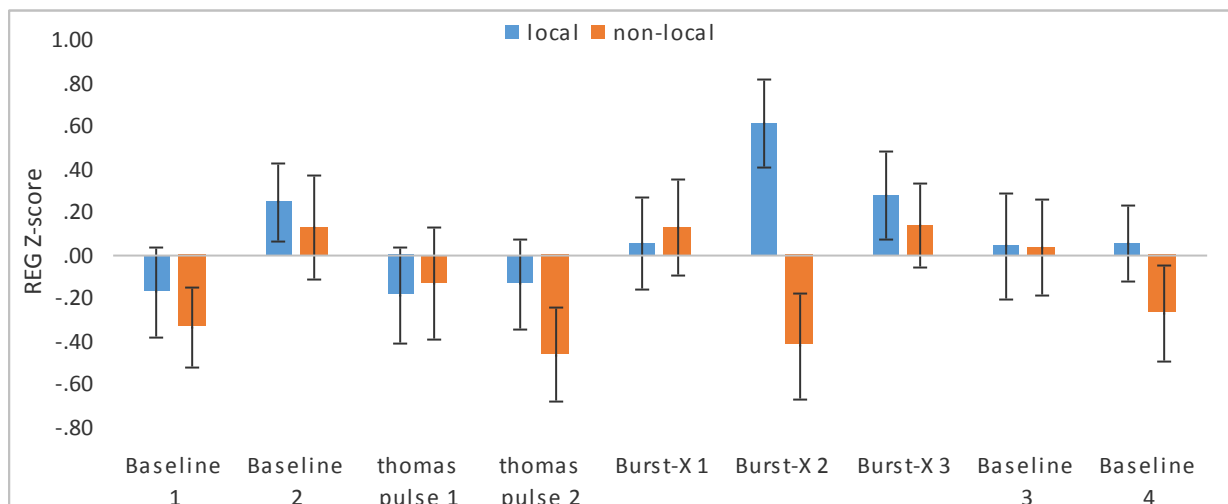


Figure 3. Means and standard deviations for the z-scores of the average numbers of 0s and 1s generated by the two REG in the local (chamber) and non-local (room 10 m away) over the various baseline and magnetic field configuration presentations. The local was an arbitrary reference. The Thomas pulse is now called the primer pulse while the burst-x pattern is called the effector pulse within which entanglement is usually manifested. Note the difference is equivalent to 1 standard deviation. Vertical bars are SEMs.

In the present study there were no human interactions directly within the entanglement processes although we obviously observed the REG and were within their proximity before and after the experiments in order to organize the equipment. Within the portion of the circularly generated fields that have been associated with excess correlations in pH and bioluminescent experiments the parity of the shift from centrality of these “random variations” was clearly apparent. Consequently the probability is very low that the effect was simply an induction artefact from the applied 1 μT magnetic fields. If these spurious inductions had occurred the deviations from random average would have been evident during the primacy field presentations and as well as during the entire interval of the effector fields. This effect did not occur.

Instead the manifestation of what we have interpreted as the consequence of the entanglement was the “excess correlation” that occurred during the second 4 min increment of the effector field presentation. During that interval there were marked and statistically significant deviations from random fluctuations of 0,1 events through the electron tunnelling through the p-n junctions in both loci. However the deviation was in the *opposite* directions as would be predicted from the consequences of an entanglement-like process. The standardized diametric displacement during this period was equivalent to about 1 standard deviation (Figure 3). This deviation is between 5 to 8 times more than the typical variation displayed by these instruments when operating continually without experimental manipulation for a month.

If two electrons as waves within the two circular arrays that generated this specific pattern of magnetic field sequences were entangled then their mass equivalents ($9.1 \cdot 10^{-31}$ kg) applied across the width of the p-n junction ($0.1 \mu\text{m}$, 10^{-7}) and multiplied by the velocity light ($3 \cdot 10^8 \text{ m} \cdot \text{s}^{-1}$) and the frequency of the universal hydrogen line ($1.42 \cdot 10^9 \text{ s}^{-1}$) results in $\sim 3.8 \cdot 10^{-20}$ J. If the functional length of the p-n junction was 20 nm, more typical of the width between neuronal plasma cell membranes, the value would be $7.6 \cdot 10^{-21}$ J. The median value would be within the 10^{-20} J range which has been shown to emerge from fundamental universal forces (Persinger, 2015). If the functional width was $\sim 1 \mu\text{m}$ the wavelength would be within the visible range.

The energy source for this excess correlation should be related to that available from the circularly generated magnetic fields. The central field strength was about $1.5 \mu\text{T}$. Consequently the square of this value divided by $2.5 \cdot 10^{-6} \text{ N} \cdot \text{A}^{-1}$ (twice the value of the magnetic permeability in vacuum) multiplied by the volume (assuming a width of 10^{-12} m^2 and a functional separation of 10^{-8} m) of 10^{-20} m^3 would be 10^{-26} J. However at least 4 min ($2.4 \cdot 10^2 \text{ s}$) was required for the effect to be displayed. The cumulative energy would have been $2.4 \cdot 10^{-24}$ J. The equivalent frequency, obtained by dividing by Planck’s constant of ($6.626 \cdot 10^{-34} \text{ J} \cdot \text{s}$) is about $3.6 \cdot 10^9 \text{ Hz}$. Considering the range of the actual volume in the p-n junction associated with the tunnelling this value is well within the range of the energy sufficient to be equivalent to the neutral hydrogen line that was required to converge with the 10^{-20} J universal unit.

References

- Aczel, A. D. (2002). *Entanglement: the greatest mystery in physics*. Raincoast Books: Vancouver.
- Ahn, J., Weinacht, T.C., Bucksbaum, P.H., (2000). Information storage and retrieval through quantum phase. *Science* 287:462-466.
- Burke, R.C., Gauthier, M.Y., Rouleau, N., Persinger, M.A., (2013). Experimental demonstration of potential entanglement of brain activity over 300 km for pairs of subjects sharing the same circular rotating, angular accelerating magnetic fields: verification by s_LORETA, QEEG measurements. *Journal of Consciousness & Exploration Research*, 4,:35-44.
- Caswell, J. M., Dotta, B. T. and Persinger, M. A. (2014). Cerebral biophoton emission as a potential factor in non-local human-machine interaction. *NeuroQuantology*, 12: 1-11.

Dotta, B.T., Mulligan, B.P., Hunter, M.D., Persinger, M.A., (2009). Evidence of macroscopic quantum entanglement during double quantitative electroencephalographic measurements of friends vs strangers. *NeuroQuantology*, 7: 548-551.

Dotta, B.T., Murugan, N.J., Karbowski, L.M., Persinger, M.A., (2013). Excessive correlated shifts in pH within distal solutions sharing phase-uncoupled angular accelerating magnetic fields: Macro-entanglement and information transfer. *International Journal of Physical Sciences*, 8: 1783-1787.

Dotta, B. T. and Persinger, M. A. (2012). "Doubling" of local photon emissions when two simultaneously, spatially separated, chemiluminescent reactions share the same magnetic field configurations. *Journal of Biophysical Chemistry*, 3, 72-80.

Eskai, L. (1958). New phenomenon in narrow Germanium P-N junction. *Physics Review*, 10: 603.

Fickler, R., Lapkiewicz, R., Plick, W.N., Krenn, M., Schaeff, C., Ramelow, S., Zeilinger, A., (2012). Quantum entanglement of high angular momenta. *Science*. 338:640-644.

Hartman, T. (1962). Tunnelling of a wave packet. *Journal of Applied Physics*. 33, 3427-33.

Hoffman, J., Krug, M., Ortegel, N., Gerard, L., Weber, M., Rosenfield, W., Weinfurter, H., (2012). Heralded entanglement between widely separated atoms. *Science*. 337:72-75.

Julsgaard, B., Kozhekin, A., Polzik, E.S., (2001). Experimental long-lived entanglement of two macroscopic objects. *Nature*. 413: 400-403.

Persinger, M. A. and Koren, S. A. (2013). Dimensional analyse of geometric products and boundary conditions of the universe: implications for a quantitative value for the latency to display entanglement. *The Open Astronomy Journal*, 6:10-13.

Persinger, M. A. (2015). Thixotropic phenomena in water: quantitative indicators of Casimir-magnetic transformations from vacuum oscillations (virtual particles). *Entropy*, 17, 6200-6212.

Persinger, M. A. and Koren, S. A. (2007). A theory of neurophysics and quantum neuroscience: implications for brain function and the limits of consciousness. *International Journal of Neuroscience*, 117, 157-175.

Symul, T., Assad, S. M., & Lam, P. K. (2011). Real time demonstration of high bitrate quantum random number generation with coherent laser light. *Applied Physics Letters*, 98: 231103-231103.

Tu, L.-C., Luo, J. and Gilles, G. T. (2005). The mass of the photon. *Reports on Progress in Physics*, 68, 77-130.

Vares, D. E., & Persinger, M. (2013). Predicting Quantum Random Events from Background Photon Density Two Days Previously: Implications for Virtual-to-Matter Determinism and Changing the Future. *Journal of Nonlocality*, 2(2).

Vaziri, A., Weihs, G. and Zeilinger, A. (2002). Experimental two-photon, three-dimensional entanglement for quantum communication. *Physical Review Letter*, 89, 240401.